

## Accepted Manuscript

Catalytic activities of Pt thin films electrodeposited onto Bi coated glassy carbon substrate toward formic acid electrooxidation

J.D. Lović, S.I. Stevanović, D.V. Tripkovic, V.M. Jovanović, R.M. Stevanović, A.V. Tripkovic, K.Dj. Popović

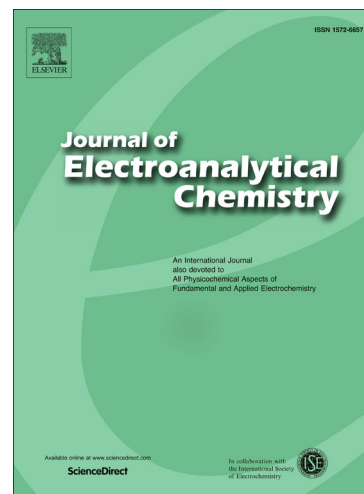
PII: S1572-6657(14)00428-7  
DOI: <http://dx.doi.org/10.1016/j.jelechem.2014.09.036>  
Reference: JEAC 1840

To appear in: *Journal of Electroanalytical Chemistry*

Received Date: 28 July 2014  
Revised Date: 24 September 2014  
Accepted Date: 29 September 2014

Please cite this article as: J.D. Lović, S.I. Stevanović, D.V. Tripkovic, V.M. Jovanović, R.M. Stevanović, A.V. Tripkovic, K.Dj. Popović, Catalytic activities of Pt thin films electrodeposited onto Bi coated glassy carbon substrate toward formic acid electrooxidation, *Journal of Electroanalytical Chemistry* (2014), doi: <http://dx.doi.org/10.1016/j.jelechem.2014.09.036>

This is a PDF file of an unedited manuscript that has been accepted for publication. As a service to our customers we are providing this early version of the manuscript. The manuscript will undergo copyediting, typesetting, and review of the resulting proof before it is published in its final form. Please note that during the production process errors may be discovered which could affect the content, and all legal disclaimers that apply to the journal pertain.



**Catalytic activities of Pt thin films electrodeposited onto Bi coated glassy carbon substrate toward formic acid electrooxidation**

J.D. Lović\*, S.I. Stevanović, D.V. Tripkovic, V.M. Jovanović, R.M. Stevanović,

A.V. Tripkovic and K.Dj. Popović

*ICTM - Center for Electrochemistry, University of Belgrade,  
Njegoševa 12, P.O.Box 473, 11000 Belgrade, Serbia*

**Abstract**

Formic acid oxidation was studied on platinum-coated bismuth deposits on glassy carbon substrate. The catalyst was prepared by a two-step process using chronocoulometry, i.e. controlled amount of Bi was electrodeposited onto glassy carbon followed by electrodeposition of Pt layer. The amount of Pt was constant while the amount of Bi vary to correspond the molar ratio of Pt:Bi = 1:0.1 or 1:1 or 1:10. AFM characterization of the electrode surface indicates that Pt is deposited preferentially on previously formed Bi particles, but cyclic voltammetry revealed Bi leaching meaning that Bi was not completely occluded by Pt. In order to obtain stable electrode surface, deposits were subjected to potential cycling up to 1.2 V vs. SCE in supporting electrolyte, prior to use as catalysts for formic acid oxidation. On this way the electrodes composed of Bi core occluded by Pt and Bi-oxide surface layers were obtained. The Pt(Bi)/GC electrodes exhibit enhanced electrocatalytic activity in comparison to Pt/GC for formic acid oxidation which depends on composition and surface morphology. High currents and onset potential shifted to negative values indicate a significant increase in direct path what is explained through ensemble effect induced by Bi-oxide species interrupting Pt domains. Electronic modification of Pt both by surface and sub-surface Bi can play some role as well. Significantly prolonged potential cycling in supporting electrolyte of previously stabilized Pt(Bi)/GC electrodes by Bi oxide, led to considerably lower Bi leaching accompanied by dissolution and redeposition of Pt and the outcome of this treatment was Pt shell over Bi core. These Pt@Bi/GC catalysts also exhibit higher activity for HCOOH oxidation in comparison to Pt/GC depending on the

---

\* Corresponding author: Jelena Lović, ICTM-Center for Electrochemistry, University of Belgrade, Njegoseva 12, 11000 Belgrade, Serbia  
Tel: +381 11 337 0389; E-mail: [JLovic@tmf.bg.ac.rs](mailto:JLovic@tmf.bg.ac.rs)

quantity of Bi remained under Pt shell, but in this case the improvement is induced solely by electronic effect of under-laying Bi.

**Key words:** Pt@Bi shell-core structure, electrochemical deposition, formic acid oxidation, AFM characterization.

## 1. Introduction

In past decades, the oxidation of small organic molecules such as formic acid and methanol has been intensively studied, for their potential use as fuels in direct fuel cells [1]. Platinum is considered one of the most efficient catalysts for the oxidation of small organic molecules. However, it is susceptible to poisoning, due to strongly adsorbed intermediates, which are formed during the oxidation processes [2,3]. It has also been shown that the electrocatalytic activity of Pt towards oxidation of small organic molecules can be improved by modification of its surface with foreign metal adatoms that should minimize the poisoning effects [4-6]. In particular, bismuth has received significant attention as Pt modifier [7,8], and different systems such as PtBi intermetallics [9-11], PtBi and Pt<sub>2</sub>Bi alloys [12,13], electrochemically co-deposited carbon supported PtBi (PtBi/C) [14] have been proposed as good catalysts for formic acid oxidation. The beneficial effect of Bi on Pt for this reaction could be due to change in Pt-Pt distance that favor direct route in formic acid oxidation [9], or to the formation of surface Bi oxides that participate in oxidation of intermediates [12], or to electronic effect by lowering the electron density of the 5d orbital, resulting in a considerable decrease of the CO binding strength to Pt [15,16], or to ensemble effect creating the appropriate size of Pt domains providing direct oxidation of HCOOH to CO<sub>2</sub> [13,17]. Depending on the preparation of the catalysts and their resulting surface composition the contribution of the above effects may vary. Also, it has been reported in the literature that Pt-Bi electrodes are not stable in the acidic media when the upper potential in cyclic voltammetry experiments was set to values higher than 0.9 V vs. Ag/AgCl. It was shown that Bi progressively released the electrode surface and Pt crystalline domains were formed on the PtBi electrode due to Bi leaching from the matrix and subsequent dissolution generating a Pt rich surface [18-20].

Among the numerous methods for synthesis of bimetallic catalysts, a new method for the preparation of noble metal coatings has been proposed whereby the surface layer of a less precious metal (Ru, Cu, Pb and Ti) is replaced with the noble metal (Pt and Pd) by

spontaneous electroless exchange, upon immersion into a complex solution of Pt or Pd ions [21-24]. Another way for forming low dimensional systems is electrodeposition of mono or multilayer metals on different substrates [25-27]. This bimetallic mono and multilayer catalyst concept has received much attention regarding its possibility to reduce the noble metal loading and maintain the activity by replacing the under-layer (bulk of the catalyst) with less noble metal. Also unlike other bimetallic catalysts where the second metal is either in the form of an adatom or as a surface alloy component, this type of catalyst allows the study of the electronic effect of second metal under-layer to the noble catalyst over-layer, as the only operating factor.

In our previous work[28], formic acid oxidation was studied on platinum-bismuth deposits on glassy carbon substrate obtained by two-step process, comprising deposition of Bi followed by deposition of Pt. Electrochemical deposition of low loading Pt layer over Bi deposits on GC electrode resulted in formation of approximately spherical clusters of Bi covered by Pt. Treatment of as prepared electrode by slow sweep up to 0.8 V *vs.* SCE leads to quantitative oxidation of Bi partially occluded by Pt, but in the same time to formation of Bi oxide, thus creating the surface composed of Pt and Bi-oxide. On this way prepared bimetallic electrode exhibits significant high activity for the reaction of formic acid oxidation as a result of well-balanced ensemble effect induced by Bi-oxide species interrupting Pt domains.

The aim of this work was to examine activity for the oxidation of formic acid of similarly prepared Pt-Bi catalyst, i.e. different amounts of Bi were electrodeposited onto GC substrate and subsequently coated with same quantity of Pt. Obtained in this way bimetallic catalysts with different ration of Pt:Bi have been preconditioned electrochemically, in contrast to our previous work, by the potential cycling in a wider potential range (up to 1.2 V *vs.* SCE and with sweep rate of 50 mV s<sup>-1</sup>) in order to explain the importance of surface composition and surface morphology for the reaction of formic acid oxidation.

## 2. Experimental Section

### 2.1. Electrode Preparation

Prior to each electrochemical experiment, the glassy carbon (GC) disc electrode (5 mm diameter) was mirror polished using Buehler silicon carbide grinding paper (P 2000-P 4000) and 1–0.05  $\mu\text{m}$  alumina. The surface was rinsed with high purity water, sonicated for 2-3 min and rinsed again. Before each deposition experiment, to ensure that the GC surface was

free of deposits, the electrode was checked by cyclic voltammetry in the potential range  $-0.25\text{ V} - 1.20\text{ V vs. SCE}$  at a scan rate  $50\text{ mV s}^{-1}$  in  $0.1\text{ M H}_2\text{SO}_4$ .

Platinum- bismuth deposits on glassy carbon substrate were prepared by a two-step process as described previously.[28] Briefly, bismuth was deposited onto the substrate from deaerated  $2\text{ mM Bi perchlorate}$  in  $0.1\text{ M H}_2\text{SO}_4$  using chronocoulometry at  $-0.1\text{ V vs. SCE}$ . The deposition potential was chosen according to quasi-steady-state potentiodynamic curve presented in Fig. 1(a). Applied deposition potential is in the region before the cathodic peak while concentration of  $\text{Bi}^{3+}$  ion offers the formation of dense and uniform Bi deposits according to 3D progressive nucleation and growth mechanism [28,29]. After Bi deposition the electrode was rinsed and transferred to the electrochemical cell containing deaerated  $1\text{ mM H}_2\text{PtCl}_6$  solution in  $0.1\text{ M H}_2\text{SO}_4$ . The proper amount of Pt was deposited using chronocoulometry at  $-0.1\text{ V vs. SCE}$  corresponding to Pt limiting current plateau in order to avoid any displacement reaction between Pt and less noble Bi and/or GC substrate, according to quasi-steady-state potentiodynamic curve presented in Fig 1(b). The amount of Pt was constant while the amount of Bi varies to correspond the molar ratio of Pt:Bi = 1:0.1 or 1:1 or 1:10. According to molar ratio electrodes were denoted as Pt(Bi01)/GC, Pt(Bi1)/GC and Pt(Bi10)/GC. The deposited charge for Pt correspond to  $10.3\text{ }\mu\text{g/cm}^2$  in all investigated samples and for Bi correspond to  $1.1\text{ }\mu\text{g cm}^{-2}$ ,  $11.02\text{ }\mu\text{g cm}^{-2}$  and  $110.2\text{ }\mu\text{g cm}^{-2}$ , respectively. For the sake of comparison Pt/GC electrode was prepared using the same electrochemical procedure and quantity corresponding to one for bimetallic electrode.

## 2.2. Electrode Characterization

### 2.2.1. *Electrochemical Characterization*

Pt(Bi)/GC electrodes, made as described in previous section, were activated by cycling potential with scan rate of  $50\text{ mV s}^{-1}$  between hydrogen and oxygen evolution in  $0.1\text{ M H}_2\text{SO}_4$  solution 8, 50 and 250 times. In order to avoid Bi redeposition, the electrode was taken out from solution at  $1.2\text{ V vs. SCE}$ .

Formic acid oxidation ( $0.125\text{ M}$ ) was investigated in  $0.1\text{ M H}_2\text{SO}_4$  solution after holding the potential for 2 min at  $-0.2\text{ V}$  by potentiodynamic (sweep rate  $50\text{ mV s}^{-1}$ ) or quasi steady-state (sweep rate  $1\text{ mV s}^{-1}$ ) measurements. The rotating speed of the disc electrode was 1500 rpm. The results are compared to Pt/GC treated in the same manner.

CO stripping measurements were performed by a pure CO bubbled through the electrolyte for 20 min while the electrode potential was kept at  $-0.2\text{ V vs. SCE}$ . After purging the electrolyte by  $\text{N}_2$  for 30 min to eliminate the dissolved CO, the adsorbed CO was oxidized

in an anodic scan at  $50 \text{ mV s}^{-1}$ . Two subsequent voltammograms were recorded to verify the completeness of the CO oxidation. Real surface area of the electrodes used was estimated by the calculation of the charge from  $\text{CO}_{\text{ads}}$  stripping voltammograms corrected for background currents (assuming  $420 \text{ } \mu\text{C cm}^{-2}$  for the CO monolayer).

All the experiments were performed in standard three-compartment electrochemical glass cells with Pt wire as the counter electrode and saturated calomel electrode as the reference electrode at room temperature. The potentials reported in the paper are expressed on the scale of the saturated calomel electrode (SCE). The electrolytes were prepared with high purity water (Millipore,  $18 \text{ M}\Omega \text{ cm}$  resistivity) and the p.a. chemicals provided by Merck. The experiments were conducted at  $295 \pm 0.5 \text{ K}$ . A VoltaLab PGZ 402 (Radiometer Analytical, Lyon, France) was employed.

### 2.2.2. Elemental Analysis

Structural examination of the catalysts was performed by EDX technique coupled by scanning electron microscopy using JEOL JSM-6610 (USA) instrument with X-Max (silicon drift) detector and SATW (super atmospheric thin window) applying  $20 \text{ keV}$ . The measurements were performed at 10 different regions of each sample.

An inductively coupled plasma–mass spectroscopy (ICP-MS) was performed to determine the quantity of Bi leached from Pt(Bi)/GC electrode during electrochemical Bi oxidation. An Agilent 7500 CE (USA) device was used. The system was calibrated using standards from AccuStandard and Bi signals were recorded for wavelengths for which no signal was observed in a pure blank solution.

### 2.2.3. Surface characterization by Atomic Force Microscopy (AFM)

Surface characterization of the catalysts was performed at room temperature in air by atomic force microscopy (AFM) using a NanoScope III A (Veeco, USA) device. Pt/GC, Bi/GC as well as of the bimetallic catalysts only Pt(Bi1)/GC electrode was analyzed. The AFM observations were carried out in the tapping mode using NanoProbes silicon nitride cantilevers with a force constant  $0.06 \text{ N m}^{-1}$ . Analysis of any surface based on AFM images was done observing a few different parts of the samples.

### 3. Results and Discussion

#### 3.1. Catalysts characterization

##### 3.1.1. AFM characterization

AFM characterization was performed for electrochemically deposited Bi alone, Pt alone and Pt(Bi) (molar ratio 1:1) deposits. AFM image presenting only Bi deposited on GC (Fig. 2(a)) reveals a structure composed of two different types of agglomerates: Smaller, spherical shaped agglomerates with pretty uniform size ( $\sim 100$  nm) are very well distributed, covering almost the entire substrate surface. Larger, elliptical shaped agglomerates ( $\sim 400$  nm) consist actually of smaller ones.

Image of electrochemically deposited Pt on GC substrate (Fig. 2(b)) shows a large difference in nucleation and growth in respect to Bi on a glassy carbon. The result suggests that Pt has a higher surface mobility compared to Bi since the agglomerates tend to form larger structures. Unlike the case of pure Bi when the substrate was almost entirely covered by two differently sized and shaped agglomerates, the morphology of the pure Pt catalyst deposited onto GC substrate consists of randomly distributed agglomerates mostly of  $\sim 300$  nm. The surface coverage in comparison to the previous sample of Bi is much lower since the substrate morphology can readily be observed. Like in the case of the prior sample the agglomerate is composed of smaller particles ( $\sim 60$  nm).

The bimetallic catalyst Pt(Bi1)/GC (Fig. 2(c)) was produced by sequential deposition of Bi followed by deposition of Pt. The image of this sample does not show bimodal particle shape and size distribution. Comparing all three images the density of bimetallic catalyst particles appears to be between that for the pure Pt (Fig. 2(b)) and pure Bi (Fig. 2(a)) and the particles resemble those for the pure Pt (Fig. 2(b)). It appears that Pt is being deposited preferentially on top of Bi crystals forming larger structures ( $\sim 700$  nm). Surface diffusion of highly mobile Pt adatoms may as well contribute to grain growth. Although it is almost impossible to determine the composition of the agglomerates from an AFM analysis alone, by comparing structures presented on the image 2(c) with AFM images for pure Bi (2(a)) and Pt (2(b)) it could be assumed that these agglomerates are most probably Pt@Bi structures consisting of Bi core surrounded by subsequently deposited Pt. EDX analysis of as-prepared Pt(Bi1)/GC catalysts (Fig. 2(e)) has confirmed that the particles are composed of both Pt and Bi with nominal molar ratio of 1:1.

Fig. 2(d) displays AFM image of Pt(Bi1)/GC catalyst after 250 potential cycles between  $-0.27$  V and  $1.2$  V vs. SCE in  $0.1$  M  $\text{H}_2\text{SO}_4$  solution. As it is shown in the image the



size of agglomerates is reduced to ~ 350 nm during the repetitive cycling, most probably due to dissolution of Bi and possible agglomeration as well as dissolution/redeposition of Pt nanoparticles. EDX data of the treated electrode (Fig. 2(f)) shows decrease in Bi quantity in Pt(Bi1)/GC electrode after potential cycling. Nevertheless, the composition obtained by EDX analysis of the treated Pt(Bi1)/GC corresponds qualitatively well to the data obtained by the ICP-MS measurements.

### 3.1.2. Electrochemical characterization

Although Pt(Bi)/GC catalysts were prepared by deposition of Bi followed by deposition of Pt, cyclic voltammetry revealed Bi leaching from the electrode surface indicating that Bi was not completely occluded by Pt. Depending on the quantity of Bi, 3 to 8 cycles are needed in order to reveal the presence of platinum (Fig. 3(a)). These basic voltammograms resemble the features characteristic for pure Pt in hydrogen adsorption/desorption region [28], but in the region of oxide formation/reduction the charge for Pt(Bi)/GC electrodes is larger. In surface oxide region the formation of larger amount of surface oxides with enhancement of Bi content and simultaneously increasing of reduction stripping peak is a consequence of Bi redox behavior which is superimposed to Pt oxide formation/reduction [8]. Larger amount of deposited Bi provides a higher coverage with oxygenated species while the rate of surface oxide reduction is the same as on Pt/GC electrode, since there is no shift of the surface oxide reduction peak.

Further potential cycling accompanied by attenuation of Bi dissolution revealed by decreasing of the charge in oxide formation/reduction region eventually after some 50 cycles leads to quasi steady state voltammograms (Fig. 3(b)). ICP-MS analysis of the solutions in which electrodes were treated indicated that depending on the Pt:Bi ratio,  $30 \pm 3\%$  of Bi was dissolved, thus approximately 70 % of Bi remained in the Pt(Bi) catalysts. Comparing the Figs. 3(a) and 3(b) it can be noticed that dissolution of Bi from the surface of Pt(Bi)/GC electrodes does not expose any additional Pt atom to the surface, which was evident from the similarity in hydrogen region of all investigated electrodes.

However, if the potential cycling is continued for additional 200 cycles, finally steady state is reached with no sign of Bi redox behavior and CVs for Pt(Bi)/GC electrodes trace that one for Pt/GC (Fig. 3(c)). ICP-MS analysis of these solutions indicated that during this expanded electrochemical treatment only additional  $15 \pm 5\%$  of Bi leached out leaving at the end about half of Bi deposited in the catalyst. Thus, while at quasi steady-state the Pt(Bi)/GC



electrodes are composed of Bi core occluded by Pt and Bi-oxide surface layers, prolonged cycling lastly results in Pt@Bi shell-core structure.

Upon this electrochemical treatment the electrochemical active surface area (EASA) decreases with an increase in number of cycles but as can be seen from Fig. 4 this decrease is more pronounced for Pt/GC (Fig. 4(a)) than for Pt(Bi1)/GC electrodes (Fig. 4(b)). Such changing of Pt EASA is attributed to the migration and agglomeration of Pt particles and particle growth as well as possible dissolution/redeposition of platinum from the surface of the catalyst. Namely, in-situ STM study of Pt nanoparticles revealed that cycling the potential to 1.0 V or higher induced Pt dissolution together with coarsening and growth of Pt nanocrystals [30]. Sugawara and co-workers [31] based on their results concluded that the loss in the electrochemically active surface area (EASA) during potential cycling was mainly due to agglomeration of Pt nanoparticles rather than electrochemical Ostwald ripening process because despite a significant Pt dissolution when cycled up to 1.4 V vs. RHE, EASA did not decrease much more than when the potential limit was 1.0 V. However, severe conditions of prolonged potential cycling up to 1.4 V vs. RHE led to a significant loss of almost 50% of the active surface area of Pt [32]. This finding is in very good agreement with the loss of the nanoparticles EASA from the TEM statistics [33]. The authors concluded that the predominant degradation mechanism was detachment of whole particles from the support and their dissolution in the electrolyte even without re-deposition [33]. So, after 50 cycles, Pt/GC catalyst lost about 35% of its initial active surface area and about one half after 250 cycles.

The loss in electrochemical surface area of Pt(Bi1)/GC catalyst is less pronounced than for Pt/GC, indicating higher stability of Pt particles deposited on Bi and surrounded by Bi-oxide in comparison to those supported on GC. However, during prolonged cycling dissolution of Bi must be followed by dissolution/redeposition of Pt since core-shell structure was finally obtained. Schematic illustration of successive step of core-shell structure formation is presented in Fig. 5.

### 3.2. CO<sub>ad</sub> stripping measurements

Oxidation of pre-adsorbed CO was examined on all investigated electrodes. The stripping voltammograms, recorded for the electrodes previously treated by 8 cycles from -0.27 V to 1.2 V in supporting electrolyte after subtraction of the background currents are given in Fig. 6. As it can be seen, the oxidation of CO<sub>ad</sub> starts at more negative potential on pure Pt/GC electrode than on bimetallic catalyst. Regarding bimetallic catalysts, less active

for  $\text{CO}_{\text{ad}}$  electrooxidation are those Pt(Bi10)/GC electrodes with higher content of Bi and Bi-oxides.

The influence of the electrochemical treatment (8, 50 and 250 cycles) on the oxidation of pre-adsorbed CO is presented in Fig. 7(a) for Pt/GC and in Fig. 7(b) for Pt(Bi1)/GC electrodes. The results presented show that the onset potential at Pt/GC is less positive than on Pt(Bi1)/GC for the same electrode treatment and while Pt(Bi1)/GC electrodes show a single peak for  $\text{CO}_{\text{ad}}$  oxidation, the developing of shoulder at lower potentials at Pt/GC previously cycled for 50 and 250 times is observed. The more severe treatment resulting in enhanced  $\text{CO}_{\text{ad}}$  oxidation for all of the electrodes. Also, again when Pt(Bi)/GC catalyst contains more Bi (Bi-oxides), therefore when it is less severely treated it is less active for oxidation of pre-adsorbed CO. Thus, it appears that quantity of Bi i.e. Bi-oxides strongly influences oxidation of  $\text{CO}_{\text{ad}}$ , but does not participate in the reaction.

Oxidative removal of CO adsorbed at Pt surfaces follows Langmuir-Hinshelwood mechanism and it is controlled by number of defects at which catalytically active OH is formed. [34-36]. Particles migration and coalescence into agglomerates induced by potential cycling produce defect-like steps and grain boundaries on the surface of coalesced particles and thus increase number of defects in comparison to smaller single particles. Smaller particles also have higher CO and oxygen binding energy due to the changed electronic structure induced by size constraint [36]. Therefore, the origin of the peak multiplicity at Pt/GC electrode is a consequence of particles aggregation [35,37]. The peak at lower potentials is associated to CO inter-particle oxidation, meaning the reaction between OH and CO species adsorbed in two different but close nanoparticles, whereas the peak at higher potentials is associated to the oxidation on the isolated nanoparticles. On the other hand, lower number of previous cycle on Pt/GC electrode induce less concentration of surface defects which are highly active for OH adsorption [38], so the CO stripping peak is positively shifted with respect to Pt/GC exposed to prolonged cycling .

Since CO does not adsorb at Bi [39], oxidation of CO occurs only on Pt sites. The sharpness and the symmetry of the  $\text{CO}_{\text{ads}}$  stripping peak generally reflects the uniformity of Pt surface [40]. As already mentioned, the Pt(Bi)/GC electrode with higher quantity of Bi in the catalyst, thus higher coverage of the surface with Bi oxide has lower activity for the oxidation of  $\text{CO}_{\text{ads}}$  and, as can be seen in Fig. 6, lower amount of the adsorbed CO. Most probably this is because Bi oxide generated during potential cycling blocks sites for CO adsorption and defect sites and leads to formation of small Pt domains. The higher coverage with the oxide reduces Pt domains and the reaction is more retarded. During potential cycling, due to Bi

leaching the coverage by Bi oxide decreases leaving larger Pt domains and most probably accompanied by particles coalescence and Pt dissolution/redeposition causes such catalyst surface morphology which facilitates  $\text{CO}_{\text{ads}}$  oxidation (Fig. 7).

The difference in onset and peak potential of  $\text{CO}_{\text{ad}}$  oxidation on Pt/GC and Pt(Bi)/GC electrodes could be ascribed also to the some electronic modification of Pt surface atoms by Bi. Namely, sites on the edge of Pt domains, being in contact with Bi phase bind  $\text{CO}_{\text{ads}}$  and  $\text{OH}_{\text{ads}}$  stronger than other Pt sites. This statement is consistent with theoretical DFT calculations presented in literature [41,42] that are based on different values of lattice constant. Since Bi possesses larger lattice constant than Pt, Pt overlayer on Bi is under a tensile strain. This results in an increase in d-band center of Pt atoms in outlayer, leading to the stronger adsorption of CO and OH on Pt thus, decreases the rate of  $\text{CO}_{\text{ad}}$  oxidation. This electronic effect has the major role in the activity for  $\text{CO}_{\text{ad}}$  oxidation on Pt(Bi)/GC electrode i.e. the catalyst obtained after 250 potential cycles since no form of Bi should be present on the surface.

### **3.3. Formic acid oxidation**

#### *3.3.1. Effect of the Bi underlayer thickness and potential cycling on the catalysts activity*

Figure 8 shows formic acid oxidation on the examined electrodes previously cycled in potential range between onset potentials of hydrogen and oxygen evolution for 8 (a), 50 (b) and 250 (c) times. This potential cycling is electrochemical treatment that determine the degree of surface reconstruction, the size of electrochemical active area and for the Pt(Bi)/GC electrodes amount of remaining Bi and Bi oxide.

Before analyzing the results obtained, it is important to recall some characteristics of polycrystalline Pt in formic acid electrooxidation, considering dual path mechanism. Dehydrogenation is assigned as the direct path, based on the oxidation of formate [43] and dehydration, i.e. indirect path, assumes formation of  $\text{CO}_{\text{ad}}$ , both generating  $\text{CO}_2$  as the final reaction product. At low potentials  $\text{HCOOH}$  oxidizes through the direct path with the simultaneous formation of  $\text{CO}_{\text{ad}}$  in indirect – dehydration path. Formation of oxygen-containing species on Pt ( $E > 0.5$  V vs. RHE [4]) enables the oxidative removal of  $\text{CO}_{\text{ad}}$ . Number of neighboring Pt sites on the electrode surface determines the reaction path, so that the dehydration path needs an ensemble of at least three adjacent Pt atoms, while the dehydrogenation path is possible on a smaller atomic ensemble [44].

Analyzing voltammograms presented in Fig. 8 reveals that fewer cycles in supporting electrolyte on all investigated electrodes provides higher activity for formic acid oxidation. The polarization curves for electrodeposited bimetallic Pt(Bi)/GC surfaces after 8 cycles in supporting solution indicate quite different behavior in comparison to Pt/GC. Figure 8(a) shows that the onset potential for the reaction on Pt(Bi10)/GC and Pt(Bi1)/GC electrode is about 200 mV less positive and on Pt(Bi01)/GC about 150 mV less positive than on Pt/GC.

The most active electrode is Pt(Bi10)/GC. The current rises up to 0.3 V and reaches a peak about 20 times higher than the peak on Pt/GC. This peak indicates predominant direct oxidation path of HCOOH to CO<sub>2</sub>, occurring on Pt sites that are not blocked by the poisoning CO<sub>ad</sub> species, while the appearance of poorly defined shoulder on the descending part of the curve signifies some participation of indirect path in the reaction as well. The currents recorded in the backward direction are higher, but the difference between forward and backward scan is not as large as on Pt/GC electrode indicating lower surface poisoning of bimetallic electrodes [45]. As the quantity of Bi in the catalyst (i.e. Bi oxide on the surface) decreases, the shoulder transforms into small peak at ~ 0.6 V on Pt(Bi1)/GC and Pt(Bi01)/GC pointing out to increased role of indirect path in the reaction (Fig. 8 (a)).

Increased number of scans in supporting solution leads to decrease in activity for formic acid oxidation for all investigated electrodes as a consequence of the surface modified morphology and surface composition (Fig. 8 (b)). The explanation is connected to Bi dissolution that is consistent with a number of potential cycling of Pt(Bi)/GC electrodes which decrease the surface oxide content producing larger Pt domains, thus encouraging the indirect path of formic acid oxidation. Also, increased number of potential scan introduces higher contribution of low-coordinated Pt atoms which are sites that preferentially adsorb oxygen-containing species [38,45]. Since oxygen-containing species do not participate in the oxidation of formate, intermediate in the dehydrogenation pathway, they act as poisoning species in direct path and decrease the activity of the catalyst.

Oxidation of formic acid on electrodes treated by 250 cycles is displayed in Fig. 8(c). As already mentioned this treatment in the case of Pt(Bi)/GC electrodes led to formation of Pt@Bi shell-core structures on GC. This means that all electrodes should have only Pt in surface layers, yet bimetallic electrodes are again more active for this reaction in comparison to similarly treated Pt/GC. The reason for enhanced activity in this case could originate only from the electronic effect of under-laying Bi core, while the different activity between bimetallic electrodes is the consequence of different thickness of Pt layers over different quantity of Bi in the core from one electrode to another.

The Fig. 8 shows that as the number of cycles increases, the features of the voltammogram progressively change due to the fact that deposited bismuth is gradually released from the electrode surface leading to a change in the Pt and Bi ratio. Based on this result, it can be pointed out that Pt(Bi)/GC surfaces treated by lower number of previous potential cycles are highly active for the HCOOH oxidation because the dehydration branch of the overall reaction is highly suppressed, which makes the amount of  $\text{CO}_{\text{ad}}$  on the surface rather low. As a result, the dehydrogenation of HCOOH molecule becomes the predominant path and the ensemble effect induced by surface oxides is crucial for their high selectivity toward dehydrogenation path.

This low loading Pt based electrode exhibits activity for the oxidation of formic acid similar to the activity of bulk  $\text{Pt}_2\text{Bi}$  alloy which has been shown to be one of the best Pt-Bi bimetallic catalysts for the oxidation of formic acid [13]. In addition, the preparation of the thin layer electrode is much easier than bulk electrodes, and consequently the electrocatalytic properties of Bi-modified Pt overlayers can be more easily studied. Moreover, the advantage of these thin layer electrodes is less consumption of noble metals and thus their lower price.

### 3.3.2. Quasi-steady state measurements

The quasi-steady state measurements for formic acid oxidation at all investigated electrodes previously cycled 50 times in potential range between -0.27 V and 1.2 V are presented in Fig. 9. The data obtained under the slow sweep conditions corroborated the difference in the activities of pure Pt/GC and Pt(Bi)/GC electrodes of different molar ratio that was found under the potentiodynamic measurements. Comparing the activities of electrodes investigated at 0.0 V it can be seen that the current densities are enhanced 7 to 25 times at different molar ratio Pt(Bi)/GC electrodes in respect to Pt/GC electrode.

The Tafel slope on Pt(Bi)/GC electrodes is about  $120 \text{ mV dec}^{-1}$ , indicating that the HCOOH oxidation takes place on surface free of  $\text{CO}_{\text{ad}}$  through dehydrogenation path, i.e. that first electron transfer is the rate-determining step, meaning that C-H bond cleavage, to form  $\text{COOH}_{\text{ad}}$ , is the slow step and determines the rate of formic acid oxidation on Pt(Bi)/GC electrodes.

The Tafel slope of about  $150 \text{ mV dec}^{-1}$  obtained during formic acid oxidation on Pt/GC electrode indicates that CO formed was adsorbed and collected on the surface slowing down the reaction rate. This means that reaction on this electrode occurs through both paths i.e. through dehydration and dehydrogenation path.

#### 4. Conclusion

Platinum coated Bi deposits, Pt(Bi), have been formed on glassy carbon (GC) electrode by a two-step process, whereby a controlled amount of Bi was electrodeposited onto the substrate and was subsequently coated with a thin Pt layer. Three different catalysts were prepared with Pt to Bi molar ratio of 1:0.1, 1:1 and 1:10.

EDX and ICP-MS analysis, AFM and electrochemical characterization revealed that initially unfinished core-shell structures were formed. Pt(Bi)/GC catalysts are not stable at potentials beyond 0.4 V vs. Ag/AgCl due to Bi leaching/dissolution from the surface which occurs through the oxidation of the less-noble metal. Electrochemical treatment by potential cycling of as prepared electrode leads to quantitative oxidation of Bi from the unprotected core forming Bi oxide simultaneously, thus creating shell composed of Pt and Bi-oxide. By prolonged cycling, the amount of surface oxides diminishes creating finally Pt@Bi shell-core structure.

These electrodes exhibit enhanced electrocatalytic activity in formic acid oxidation in comparison to Pt/GC electrode treated on the similar way, both during voltammetric and quasi steady-state experiments. It was shown that the activity of bimetallic electrodes in formic acid oxidation depends on surface composition and surface morphology. A gradual increase of anodic current up to 25 times compared to Pt/GC as well as the shift of the onset potentials up to 0.2 V to more negative values, observed by increasing Bi content in the catalyst indicates turnover of the reaction more to direct path (dehydrogenation) caused by of Bi and Bi oxide. This behavior is explained primarily by ensemble effect induced by surface Bi oxides interrupting Pt domains but to some extent could also be attributed to the influence of the under-lying Bi onto the Pt surface layer, affecting the extent of poison adsorption on the Pt. Due to the electronic effect of this under-laying Bi, Pt@Bi/GC (shell-core) catalysts with only Pt in surface layers exhibit somewhat enhanced activity which depends on Pt layer thickness determined by the quantity of Bi in the core.

In this way by controlling the thickness of Bi and Pt layers using electrochemical techniques it was possible to improve the electrocatalytical properties of Pt(Bi)/GC in HCOOH oxidation and to create the low loading Pt based catalyst with the comparable activity to the bulk metal alloy.

***Acknowledgements***

This work was financially supported by the Ministry of Education and Science, Republic of Serbia, Contract No. H-172060.

ACCEPTED MANUSCRIPT



**Figure captions:**

- Fig. 1: Polarization curve for deposition of Bi onto GC substrate (a) and Pt on GC substrate (b) in 0.1 M H<sub>2</sub>SO<sub>4</sub> solution. Scan rate: 1 mV s<sup>-1</sup>.
- Fig. 2: AFM images of Bi (a), Pt (b), as prepared Pt(Bi1) (c) and Pt(Bi1) treated 250 cycles (d) deposits on GC substrate (2x2x1 μm). EDX data for Pt(Bi1)/GC electrode before (e) and after electrochemical treatment (f).
- Fig. 3: Cyclic voltammograms of Pt/GC and Pt(Bi)/GC electrodes in 0.1 M H<sub>2</sub>SO<sub>4</sub> recorded after 8 (a), 50 (b) and 250 (c) cycles. ω = 1500 rpm. Scan rate: 50 mV s<sup>-1</sup>.
- Fig. 4: Comparison of basic voltammograms for Pt/GC (a) and Pt(Bi1)/GC electrode (b) recorded after 8, 50 and 250 cycles in 0.1 M H<sub>2</sub>SO<sub>4</sub> solution. ω = 1500 rpm. Scan rate: 50 mV s<sup>-1</sup>.
- Fig. 5: Schematic illustration of the stages in Pt@Bi shell- core electrochemical formation.
- Fig. 6: CO stripping voltammograms (first positive going sweeps) recorded at Pt/GC and Pt(Bi)/GC electrodes previously cycled 8 times in 0.1 M H<sub>2</sub>SO<sub>4</sub> solution, corrected for background current. ω = 1500 rpm. Scan rate: 50 mV s<sup>-1</sup>.
- Fig. 7: CO stripping voltammograms (first positive going sweeps) recorded at electrodes previously cycled 8, 50 and 250 times in 0.1 M H<sub>2</sub>SO<sub>4</sub> solution, corrected for background current: (a) Pt/GC and (b) Pt(Bi1)/GC. ω = 1500 rpm. Scan rate: 50 mVs<sup>-1</sup>
- Fig. 8: Cyclic voltammograms for oxidation of 0.125 M HCOOH in 0.1 M H<sub>2</sub>SO<sub>4</sub> recorded on Pt/GC and Pt(Bi)/GC electrodes after 8 (a), 50 (b) and 250 (c) cycles in 0.1 M H<sub>2</sub>SO<sub>4</sub>. ω = 1500 rpm. Scan rate: 50 mV s<sup>-1</sup>.
- Fig. 9: Tafel plots for the oxidation of 0.125 M HCOOH in 0.1 M H<sub>2</sub>SO<sub>4</sub> solution on Pt/GC and Pt(Bi)/GC electrodes previously cycled 50 times in 0.1 M H<sub>2</sub>SO<sub>4</sub> solution. ω = 1500 rpm. Scan rate: 1 mV s<sup>-1</sup>.

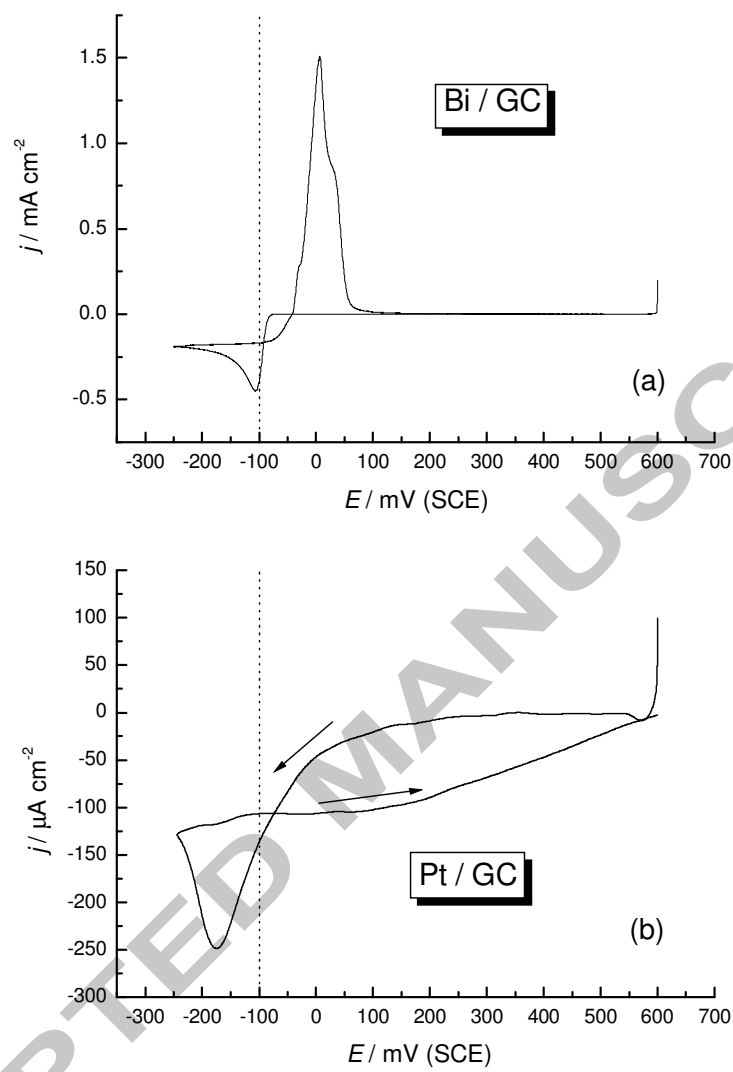


Fig.1

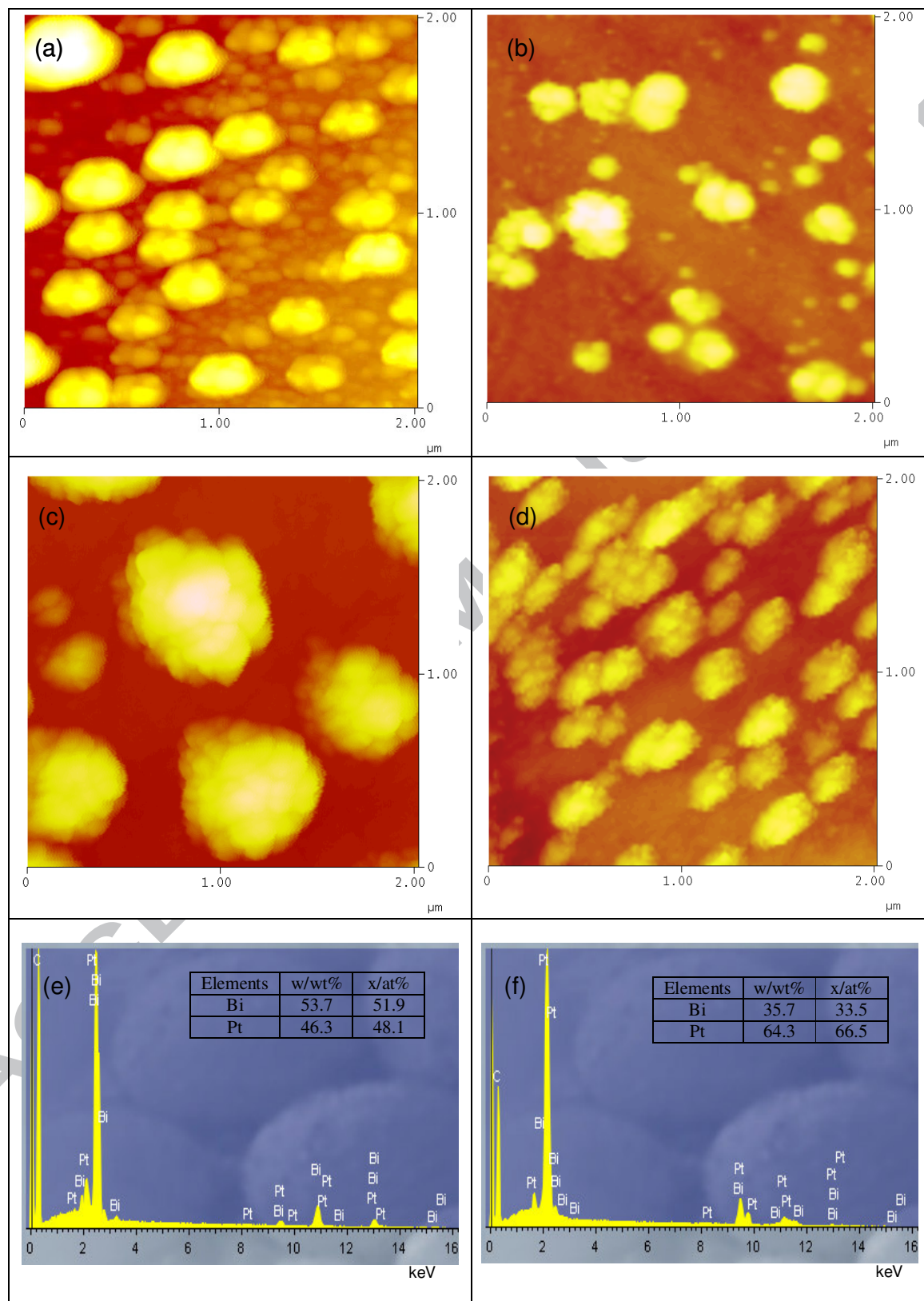


Fig.2

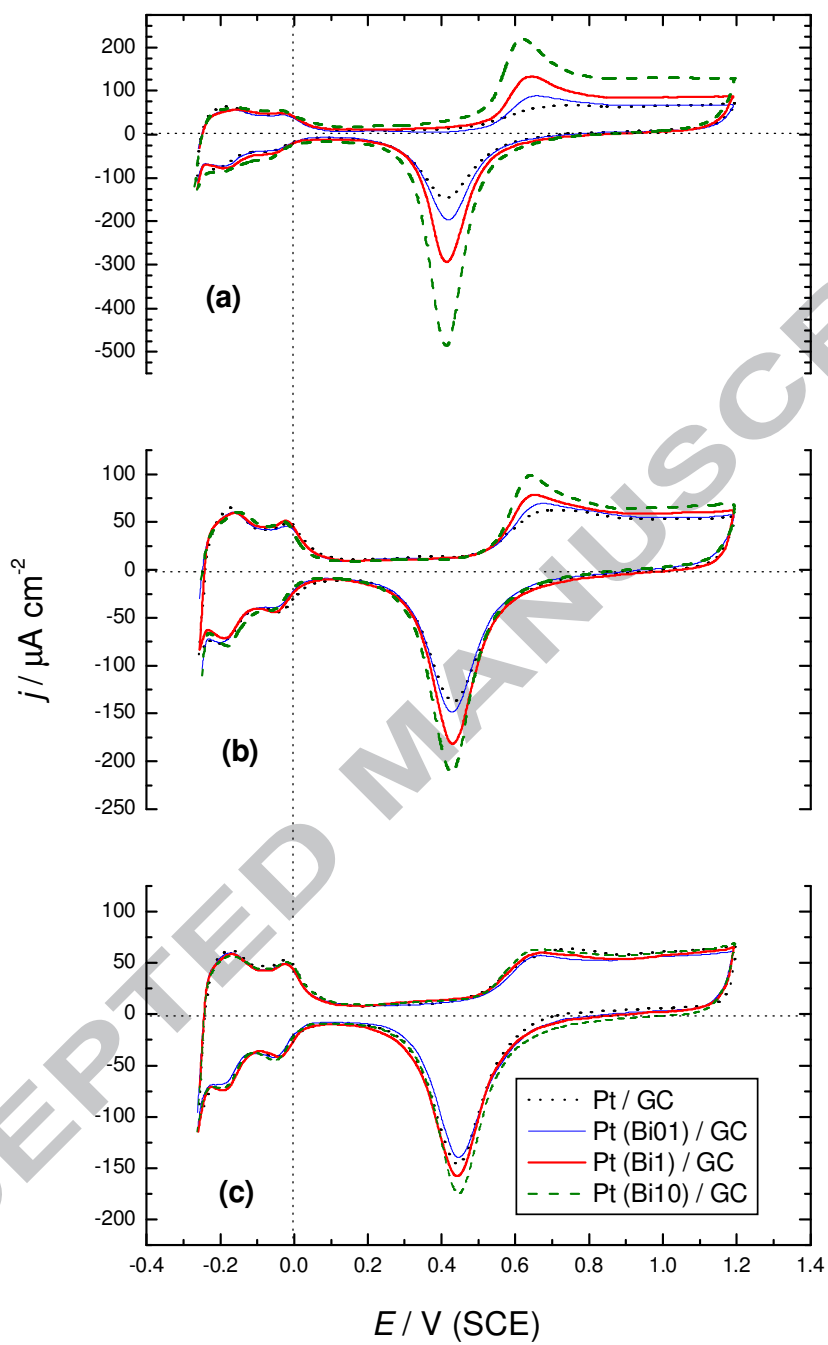


Fig.3

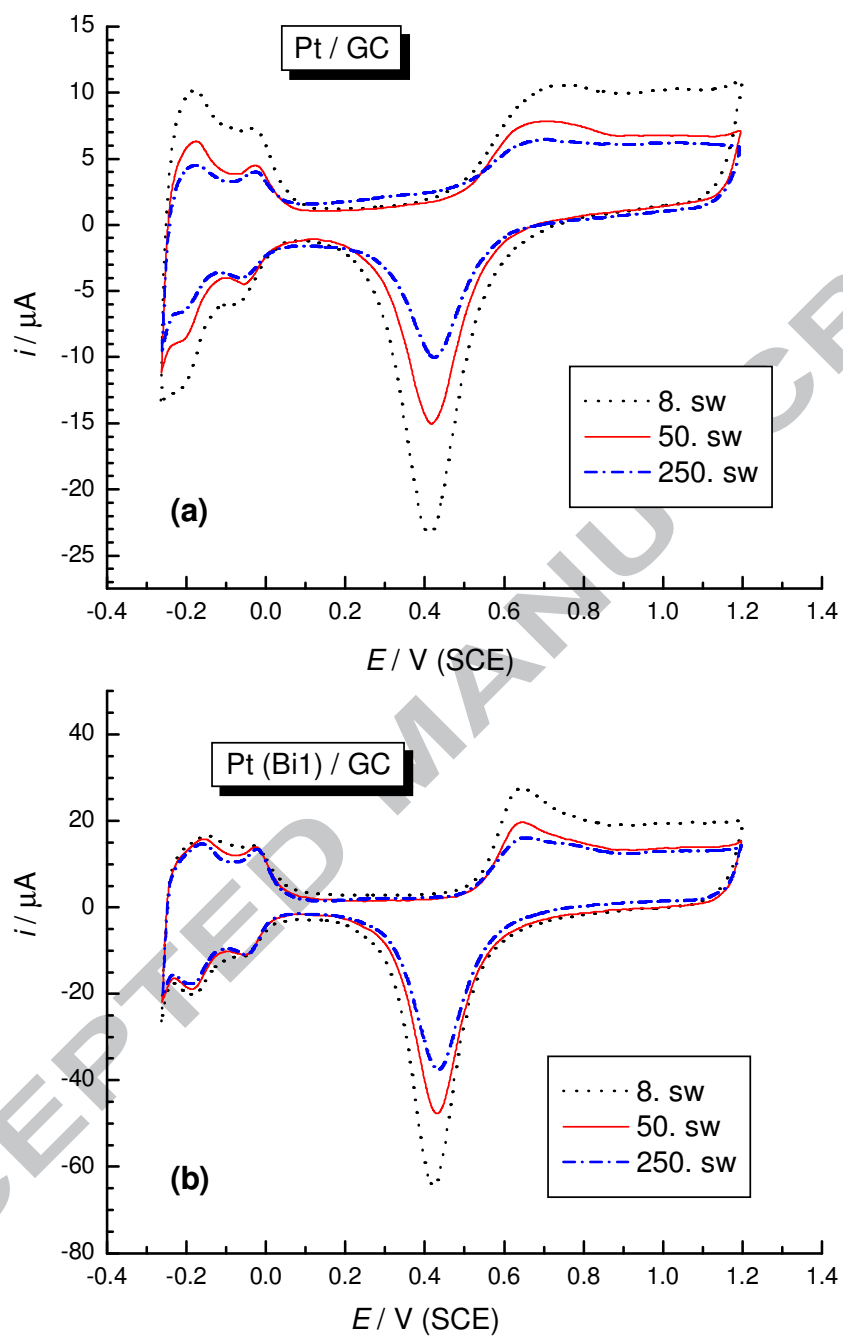


Fig.4

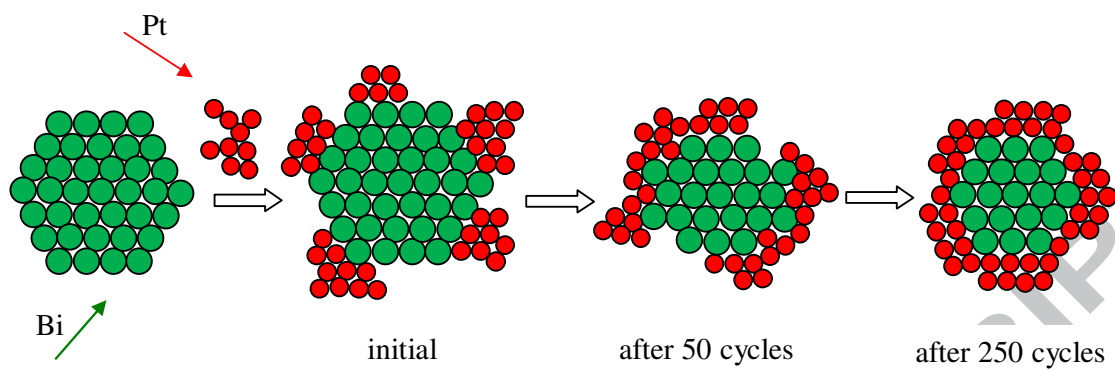


Fig.5

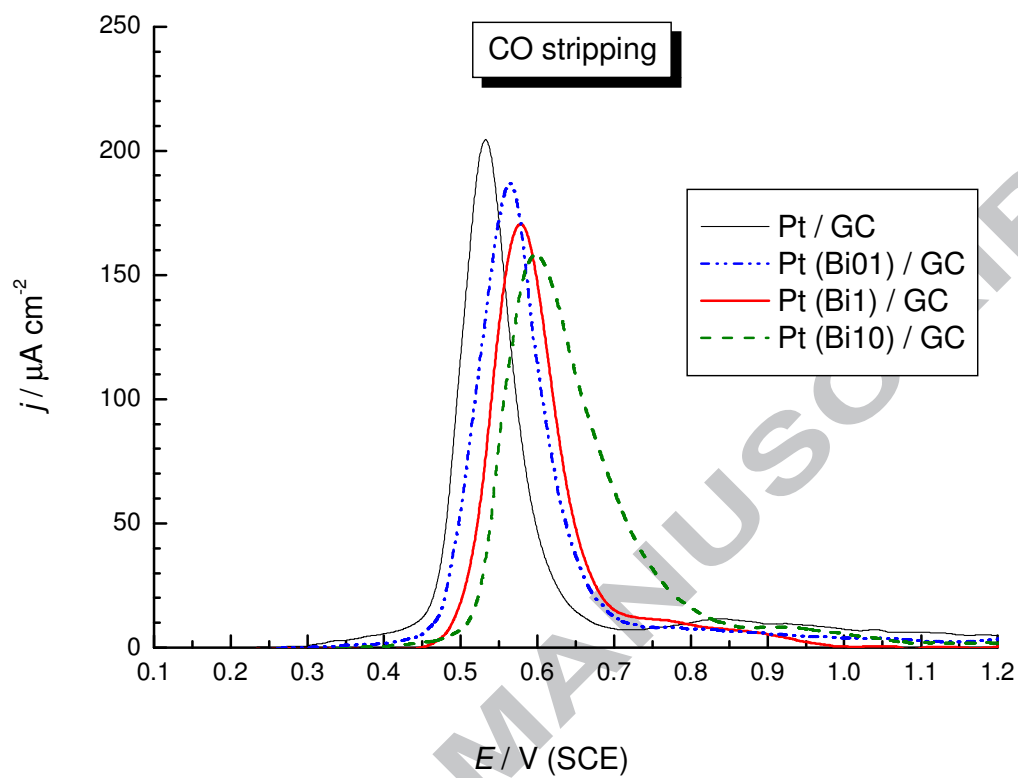


Fig.6



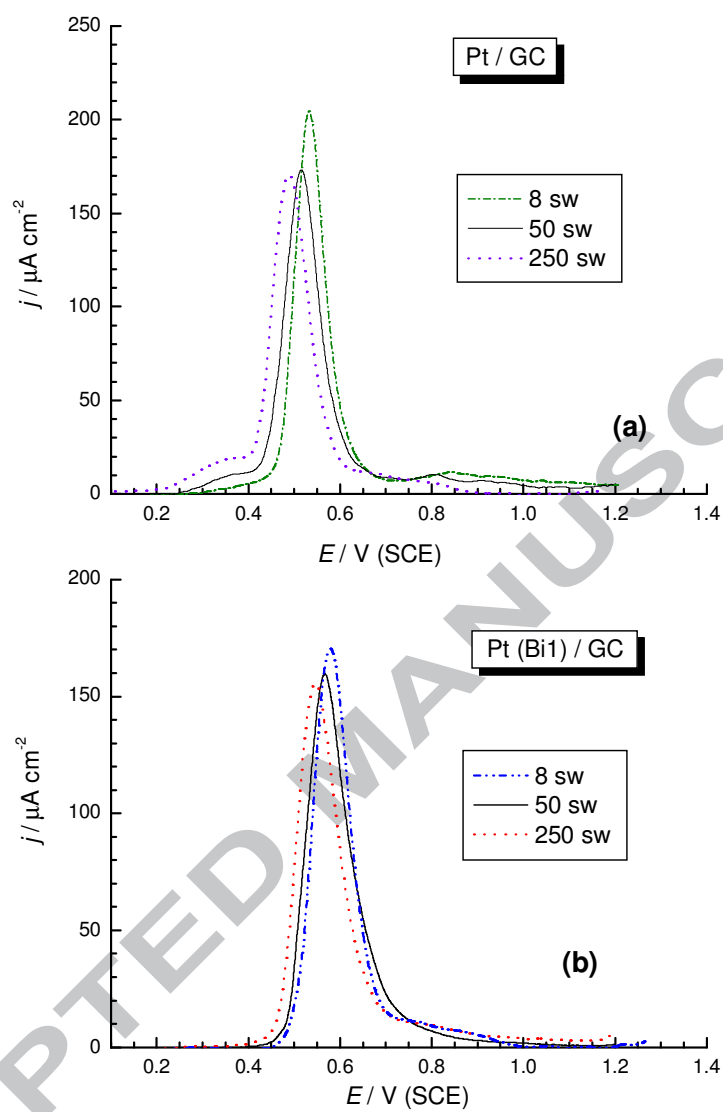


Fig.7

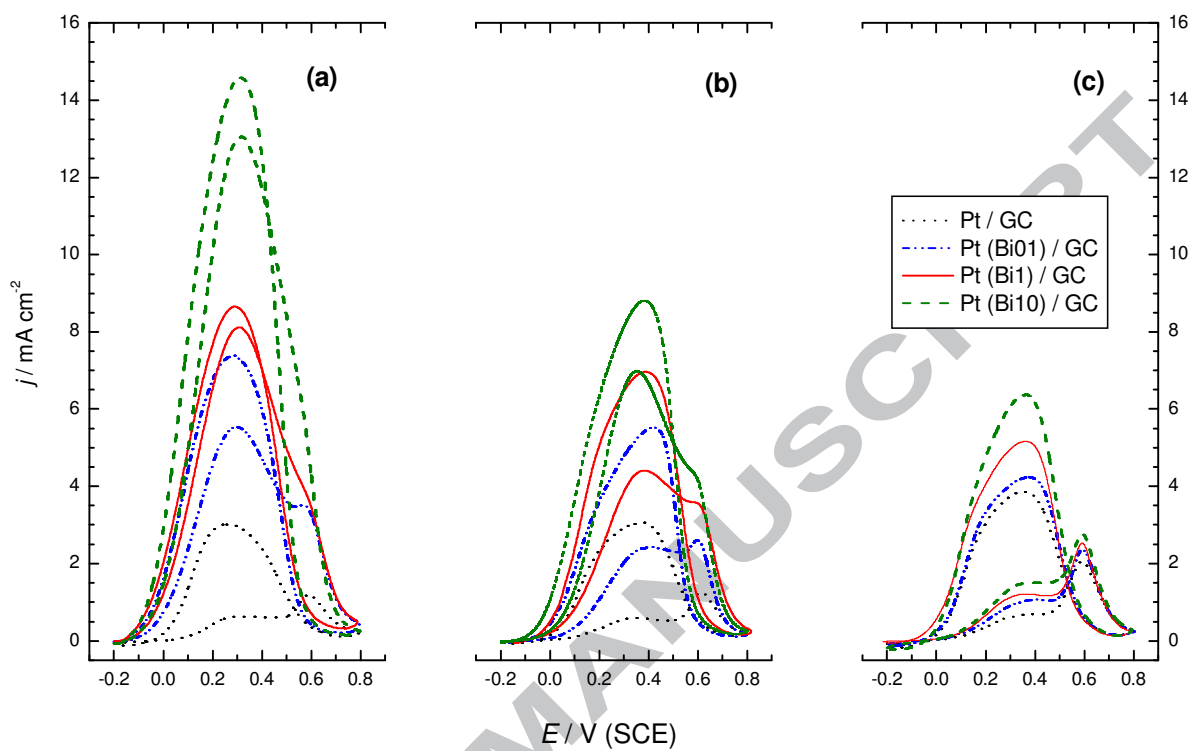


Fig.8

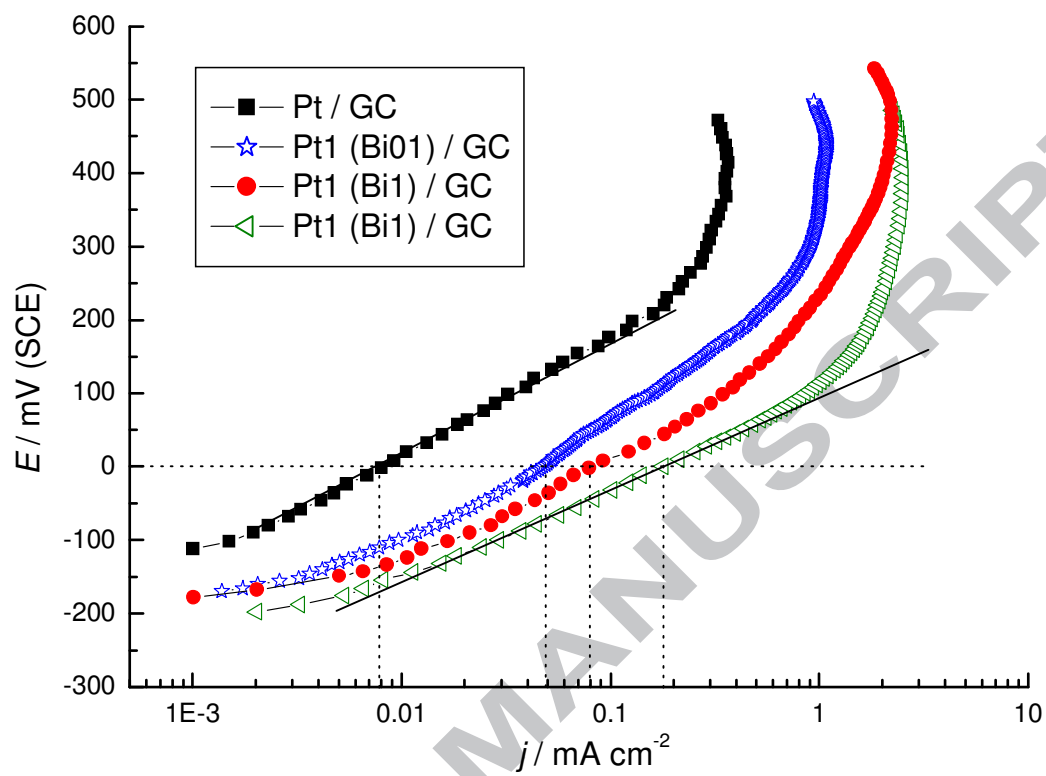


Fig.9

## References:

1. R. Parsons, T. VanderNoot, **The oxidation of small organic molecules: A survey of recent fuel cell related research**, *J. Electroanal. Chem.*, 257 (1988) 9-45.
2. J.M. Feliu and E. Herrero in Handbook of Fuel Cells - Fundamentals, Technology and Applications, Edited by W. Vielstich, H. A. Gasteiger, A. Lamm. Volume 2: Electrocatalysis, 2003, John Wiley & Sons, N.Y., p. 625.
3. A. Capon, R. Parsons, **The oxidation of formic acid at noble metal electrodes Part III. Intermediates and mechanism on platinum electrodes**, *J. Electroanal. Chem.*, 45 (1973) 205-231.
4. N.M. Markovic, P.N. Ross Jr., **Surface science studies of model fuel cell electrocatalysis**, *Surf. Sci. Rep.*, 45 (2002) 117-229.
5. L.J. Zhang, Z.Y. Wang, D.G. Xia, **Bimetallic PtPb for formic acid electro-oxidation**, *J. Alloys and Compounds*, 426 (2006) 268-271.
6. W. Liu, J. Huang, **Electro-oxidation of formic acid on carbon supported Pt-Os catalyst**, *J. Power Sources*, 189 (2009) 1012-1015.
7. E. Herrero, A. Fernandez-Vega, J.M. Feliu, A. Aldaz, **Poison formation reaction from formic acid and methanol on Pt(111) electrodes modified by irreversibly adsorbed Bi and As**, *J. Electroanal. Chem.*, 350 (1993) 73-88.
8. B.-J. Kim, K. Kwon, C. K. Rhee, J. Han, T.-H. Lim, **Modification of Pt nanoelectrodes dispersed on carbon support using irreversible adsorption of Bi to enhance formic acid oxidation**, *Electrochim. Acta*, 53 (2008) 7744-7750.
9. E. Casado-Rivera, Z. Gal, A.C.D. Angelo, C. Lind, F.J. DiSalvo, H.D. Abruna, **Electrocatalytic oxidation of formic acid at an ordered intermetallic PtBi surface**, *ChemPhysChem.*, 4 (2003) 193-199.
10. D. Volpe, E. Casado-Rivera, L. Alden, C. Lind, K. Hagerdon, C. Downie, C. Korzniewski, F.J. DiSalvo, H.D. Abruna, **Surface treatment effects on the electrocatalytic activity and characterization of intermetallic phases**, *J. Electrochem. Soc.*, 151(2004) A971-A977.
11. J. Sanabria-Chinchilla, H. Abe, F. J. DiSalvo, H. D. Abruna, **Surface characterization of ordered intermetallic PtBi(001) surfaces by ultra-high vacuum-electrochemistry (UHV-EC)**, *Surf. Sci.*, 602 (2008) 1830-1836.
12. A.V. Tripković, K.Dj. Popović, R.M. Stevanović, R. Socha, A. Kowal, **Activity of a PtBi alloy in the electrochemical oxidation of formic acid**, *Electrochem. Comm.*, 8 (2006) 1492-1498.
13. J.D. Lović, M.D. Obradović, D.V. Tripković, K.Dj. Popović, V.M. Jovanović, S.Lj. Gojković, A.V. Tripković, **High activity and stability of Pt<sub>2</sub>Bi catalyst in formic acid oxidation**, *Electrocatalysis*, 3 (2012) 346-352.
14. X. Yu, P.G. Pickup, **Carbon supported PtBi catalysts for direct formic acid fuel cells**, *Electrochim. Acta*, 56 (2011) 4037-4043.
15. L.R. Alden, D.K. Han, F. Matsumoto, H.D. Abruna, F.J. DiSalvo, **Intermetallic PtPb nanoparticles prepared by sodium naphthalide reduction of metal-organic precursors: electrocatalytic oxidation of formic acid**, *Chem. Mater.*, 18 (2006) 5591-5596.
16. N. de-los-Santos-Alvarez, L.R. Alden, E. Rus, H. Wang, F.J. DiSalvo, H.D. Abruna, **CO tolerance of ordered intermetallic phases**, *J. Electroanal. Chem.*, 626 (2009) 14-22.
17. A. Lopez-Cudero, F. J. Vidal-Iglesias, J. Solla-Gullon, E. Herrero, A. Aldaz, J. M. Feliu, **Formic acid electrooxidation on Bi-modified polyoriented and preferential (111) Pt nanoparticles**, *Phys. Chem. Chem. Phys.*, 11 (2009) 416-424.

18. S. Daniele, S. Bergamin, **Preparation and voltammetric characterisation of bismuth-modified mesoporous platinum microelectrodes. Application to the electrooxidation of formic acid**, *Electrochem. Comm.* 9 (2007) 1388-1393.
19. D.R. Blasini, D. Rochefort, E. Fachini, L.R. Alden, F.J. DiSalvo, C.R. Cabrera, H.D. Abruna, **Surface composition of ordered intermetallic compounds PtBi and PtPb**, *Surf. Sci.*, 600 (2006) 2670-2680.
20. Y. Liu, M.A. Lowe, F.J. DiSalvo, H.D. Abruna, **Kinetic stabilization of ordered intermetallic phases as fuel cell anode materials**, *J. Phys. Chem. C*, 114 (2010) 14929-14938.
21. S.R. Branković, J.X. Wang, R.R. Adžić, **Metal monolayer deposition by replacement of metal adlayers on electrode surfaces**, *Surf. Sci.Lett.*, 747 (2001) L173-L179.
22. J. Zhang, F. H. B. Lima, M. H. Shao, K. Sasaki, J. X. Wang, J. Hanson, R. R. Adžić, **Platinum monolayer on nonnoble metal-noble metal core-shell nanoparticle electrocatalysts for O<sub>2</sub> reduction**, *J. Phys. Chem. B*, 109 (2005) 22701-22704.
23. J. Zhang, M.B. Vukmirović, K. Sasaki, A. U. Nilekar, M. Mavrikakis, R. R. Adžić, **Mixed-metal Pt monolayer electrocatalysts for enhanced oxygen reduction kinetics**, *J. Am. Chem. Soc.*, 127 (2005) 12480-12481.
24. S. Papadimitriou, S. Armyanov, E. Valova, A. Hubin, O. Steenhaut, E. Pavlidou, G. Kokkinidis, S. Sotiropoulos, **Methanol oxidation at Pt-Cu, Pt-Ni, and Pt-Co electrode coatings prepared by a galvanic replacement process**, *J. Phys. Chem. C*, 114 (2010) 5217-5223.
25. R.G. Freitas, E.C. Pereira, **Giant multilayer electrocatalytic effect investigation on Pt/Bi/Pt nanostructured electrodes towards CO and methanol electrooxidation**, *Electrochim. Acta*, 55 (2010) 7622-7627.
26. R.G. Freitas, E.P. Antunes, E.C. Pereira, **CO and methanol electrooxidation on Pt/Ir/Pt multilayers electrodes**, *Electrochim. Acta*, 54 (2009) 1999-2003.
27. A. Tegou, S. Papadimitriou, G. Kokkinidis, S. Sotiropoulos, **A rotating disc electrode study of oxygen reduction at platinised nickel and cobalt coatings**, *J. Solid State Electrochem*, 14 (2010) 175-184.
28. J.D. Lović, S.I. Stevanović, D.V. Tripković, V.V. Tripković, R.M. Stevanović, K.Dj. Popović, V.M. Jovanović, **Formic acid oxidation at platinum-bismuth clusters**, *J. Electrochem. Soc.*, 161 (2014) H547-H554.
29. M. Yang, Z. Hu, **Electrodeposition of bismuth onto glassy carbon electrodes from nitrate solutions**, *J. Electroanal. Chem.*, 583 (2005) 46-55.
30. Q. Xu, E. Kreidler, D.O. Wipf, T. He, **In situ electrochemical STM study of potential-induced coarsening and corrosion of platinum nanocrystals**, *J. Electrochem. Soc.*, 155 (2008) B228-B231.
31. Y. Sugawara, A.P. Yadav, A. Nishikata, T. Tsuru, **Dissolution and surface area loss of platinum nanoparticles under potential cycling**, *J. Electroanal. Chem.*, 662 (2011) 379-383.
32. K. Hartl, M. Nesselberger, K.J.J. Mayrhofer, S. Kunz, F.F. Schweinberger, G.H. Kwon, M. Hanzlik, U. Heiz, M. Arenz, **Electrochemically induced nanocluster migration**, *Electrochim. Acta*, 56 (2010) 810-816.
33. K.J.J. Mayrhofer, J.C. Meier, S.J. Ashton, G.K.H. Wiberg, F. Kraus, M. Hanzlik, M. Arenz, **Fuel cell catalyst degradation on the nanoscale**, *Electrochem. Commun.*, 10 (2008) 1144-1147.

- 
34. M. Arenz, K.J.J. Mayrhofer, V. Stamenković, B.B. Blizanac, T. Tomoyuki, P.N. Ross, N.M. Marković, **The effect of the particle size on the kinetics of CO electrooxidation on high surface area Pt catalysts**, *J. Am. Chem. Soc.*, 127 (2005) 6819-6829.
35. A. Lopez-Cudero, J. Solla-Gullon, E. Herrero, A. Aldaz, J.M. Feliu, **CO electrooxidation on carbon supported platinum nanoparticles: Effect of aggregation**, *J. Electroanal. Chem.*, 644 (2010) 117-126.
36. F. Maillard, S. Schreier, M. Hanzlik, E.R. Savinova, S. Weinkauff, U. Stimming, **Influence of particle agglomeration on the catalytic activity of carbon-supported Pt nanoparticles in CO monolayer oxidation**, *Phys. Chem. Chem. Phys.*, 7 (2005) 385-393.
37. E.G. Ciapina, S.F. Santos, E.R. Gonzalez, **The electrooxidation of carbon monoxide on unsupported Pt agglomerates**, *J. Electroanal. Chem.*, 644 (2010) 132-143.
38. D. Tripković, S. Stevanović, A. Tripković, A. Kowal, V.M. Jovanović, **Structural effect in electrocatalysis: Formic acid oxidation on Pt electrodeposited on glassy carbon support**, *J. Electrochem. Soc.*, 155 (2008) B281-B289.
39. T.J. Schmidt, B.N. Grgur, R.J. Behm, N.M. Marković, P.N. Ross, Jr., **Bi adsorption on Pt(111) in perchloric acid solution: A rotating ring-disk electrode and XPS study**, *Phys. Chem. Chem. Phys.*, 2 (2000) 4379-4386.
40. N.P. Lebedeva, M.T.M. Koper, E. Herrero, J.M. Feliu, R.A. van Santen, **Cooxidation on stepped Pt[n(111)x(111)] electrodes**, *J. Electroanal. Chem.*, 487 (2000) 37-44.
41. J.R. Kitchin, J.K. Nørskov, M.A. Barteau, J.G. Chen, **Modification of the surface electronic and chemical properties of Pt(111) by subsurface 3d transition metals**, *J. Chem. Phys.*, 120 (2004) 10240-10246.
42. J.R. Kitchin, J.K. Nørskov, M.A. Barteau, J.G. Chen, **Role of strain and ligand effects in the modification of the electronic and chemical properties of bimetallic surfaces**, *Phys. Review Lett.*, 93 (2004) 156801-1-156801-4.
43. A. Miki, S. Ye, M. Osawa, **Surface-enhanced IR absorption on platinum nanoparticles: an application to real-time monitoring of electrocatalytic reactions**, *Chem. Commun.*, (2002) 1500-1501 .
44. A. Cuesta, M. Escudero, B. Lanova, H. Baltruschat, **Cyclic voltammetry, FTIRS and DEMS study of the electrooxidation of carbon monoxide, formic acid and methanol on cyanide-modified Pt(111) electrodes**, *Langmuir*, 25 (2009) 6500-6507.
45. A. Lopez-Cudero, F.J. Vidal-Iglesias, J. Solla-Gullon, E. Herreo, A. Aldaz, J.M. Feliu, **Formic acid electrooxidation on Bi-modified Pt(110) single crystal electrodes**, *J. Electroanal. Chem.*, 637 (2009) 63-71.

---

**Highlights:**

- Platinum coated Bi deposits on GC electrode prepared by a two-step process.
- Electrochemical treatment creates shell composed of Pt and Bi-oxide.
- Pt(Bi)/GC compare to Pt/GC exhibit enhanced activity in formic acid oxidation.
- Improved activity in formic acid oxidation with increasing Bi content.